

# Ferrocene Doping in Horizontal Hydride Vapor Phase Epitaxy

Martin Klein

*In order to produce semi-insulating, thick layers of gallium nitride we try to incorporate iron into our hydride vapor phase grown material. As past experiments have shown, a solid iron source inside the reactor is not adequate in terms of controllability and purity. Therefore our reactor has been upgraded with a gaseous ferrocene source. This article demonstrates first promising results and shows the current problems together with some possibilities to solve them.*

## 1. Introduction

Gallium nitride (GaN) is a very promising material for the production of high power, high frequency transistor devices [1,2]. However, the standard material grown in metal organic vapor phase epitaxial (MOVPE) and hydride vapor phase epitaxial (HVPE) machines suffer from comparably high unintentional n-type doping levels. These high doping levels favor the formation of parasitic, conductive channels, interfering with the on/off ratio of the device. As a simple and carefree way to get rid of excess carriers we are trying to incorporate deep level traps into our thick GaN buffers grown by HVPE. The source element of our choice to achieve this is iron [3]. In former studies we have described the doping of our HVPE grown GaN by creating iron-chloride from a solid iron source inside the reactor [4]. However, controllability and purity of the source did not meet our requirements in the end. In general, gaseous sources are known to perform very well in both of these regimes. Indeed, ferrocene is well established as a metalorganic precursor for iron doping in MOVPE [5] and has also been tested in HVPE growth of GaN before [6]. Because of the horizontal hot-wall design of our reactor, special care has to be taken in the design of the doping line. With our project partner Aixtron we were able to overcome these specific problems and successfully added a ferrocene source to our setup.

## 2. Design of the Doping Line

We expected, that for the high amount of unintentional dopants in our standard layers, we need a lot of incorporated iron for compensation. Owing to the low vapor pressure of ferrocene, this can only be realized by heating the bubbler. The standard implementation of such a heating consists of a temperature controlled bath with a heat transfer medium which contains the bubbler and keeps it at the desired temperature. During the transport to the reactor we must not allow the hot gas to cool down, else we risk depositions inside

the transport line. The solution is a line heating, reaching from the last flow controller to the reactor inlet. For better controlability of the doping level, a dilution stage has been chosen for use with the bubbler setup (Fig. 1). The setup can be supplied by either nitrogen or hydrogen for different operation purposes.

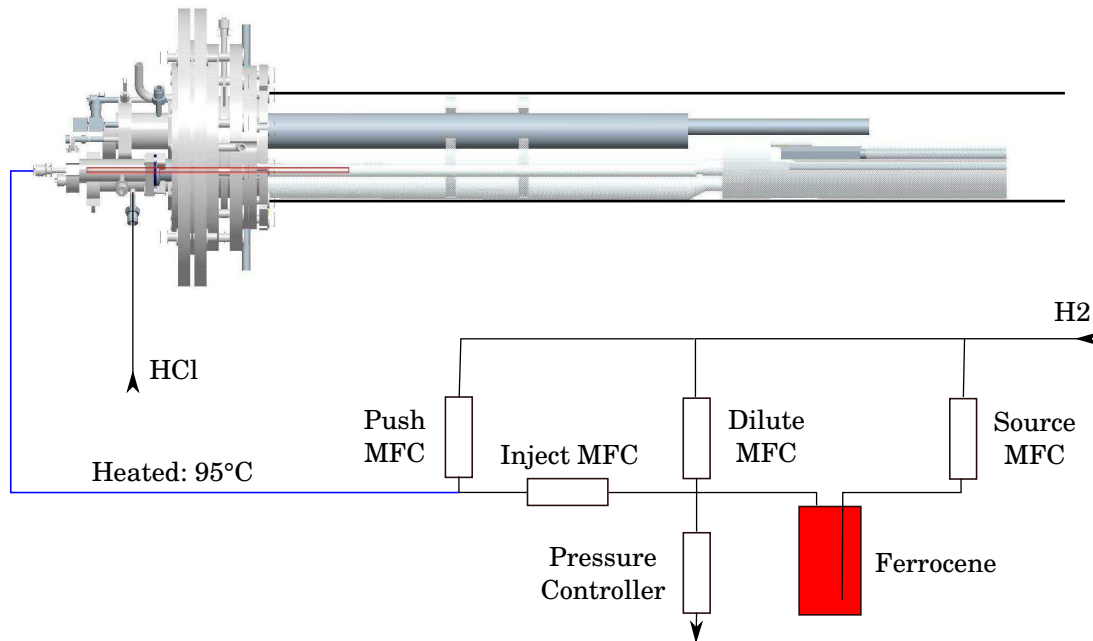


**Fig. 1:** Reactor source flange and bubbler setup with gas flow controllers. Gas flow from hydrogen source to the growth zone: the bubbler is fed with gas by the source MFC. The hereby enriched carrier gas can be diluted and sent towards the reactor via the inject MFC. In order to regulate the pressure, the pressure controller sends surplus gas to the vent. For faster transport, the injected gas can be filled up with the push MFC. After the heated line from the push MFC to the reactor, a small tube guides the gas into the reactor. HCl is provided coaxially through the same flange for creation of iron chloride inside the heated zone.

From literature we know that ferrocene decomposes at temperatures above  $500\text{ }^{\circ}\text{C}$  [7]. Because of our HVPE being a hot-wall reactor, the ferrocene has to be transported through thermal zones with temperatures of up to  $1100\text{ }^{\circ}\text{C}$  before it reaches the growth zone. To prevent the ferrocene from decomposing prematurely and forming an iron deposition on the glass parts, we add hydrogen chloride (HCl) to the carrier gas/ferrocene mixture. Ferrocene together with HCl forms the thermally stable gaseous species iron-(II)-chloride and iron-(III)-chloride at elevated temperatures, which then can be transported to the growth zone.

With the new line installed, the reactor inlet flange is almost at its maximum functionality (Fig. 2 (top)). For the purpose of introducing the new source gases into the reactor, the small 25 mm flange between the Ga-channel and the ammonia inlet has been chosen. On top of this flange, a short steel tube with a side inlet has been mounted (Fig. 2 (bottom)). Inside this tube we find a spring load mechanism that fastens the glass tube reaching into the reactor. At the end of the steel tube we find another 25 mm flange that is sealed by

a lid, incorporating an ultra-torr fitting on the inside and a VCR port on the outside. The ultra-torr holds a 8 mm glass tube that coaxially reaches into the bigger glass tube inside the reactor and transports the carrier gas/ferrocene mixture. The sideport is used to introduce HCl gas into the gap between the two coaxial glass tubes.

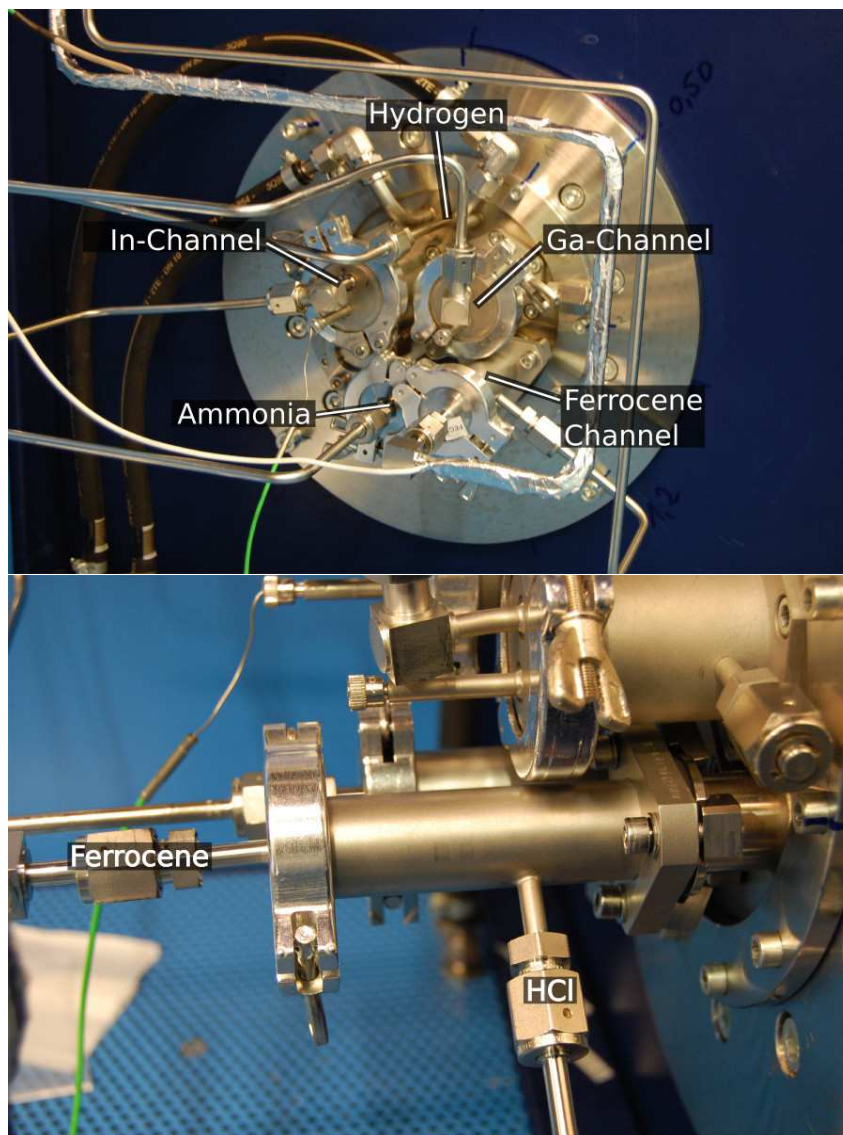


**Fig. 2:** Photographs of the reactor flange with all gas inlets (top) and the ferrocene inlet in detail (bottom).

Inside the reactor the spring loaded glass tube transports the gases towards a newly designed gas-mixing-chamber, where it is guided to a small showerhead on top of the growth zone. The 8 mm tube only covers some small part of this length. The end of this inner glass tube marks the mixing zone for the carrier gas/ferrocene mixture with the HCl and therefore defines the reaction temperature of these two species.

The small showerhead currently possesses 8 holes with a diameter of about 2 mm, dis-

tributed evenly over the 3" of the rotation tray, which is holding the sample substrate. By this design a uniform distribution of the dopant gas over the rotating wafer is expected.

### 3. Estimating the Operating Parameters

The parameters that influence the mass transport of the source material in a bubbler setup are the bubbler pressure, the carrier gas flux through the bubbler and the temperature of the material inside the bubbler.

Our HVPE growth is currently established at a reactor pressure of 900 hPa. In order for the ferrocene doping line to be functional, the bubbler pressure has to be kept above the reactor pressure. Therefore the bubbler pressure can currently not be set to values below 950 hPa. It is generally possible to establish growth at lower pressure values but this would require extensive optimization efforts.

Concerning the possible flux through the doping line, we conducted some ammonium-chloride haze experiments: in order to conduct such an experiment, we have filled the reactor with ammonia and subsequently supplied HCl flux to the source lines that are to be examined. At the position where the ammonia comes into contact with HCl, ammonium-chloride is formed. At room temperature, the ammonium chloride appears as a white haze and can be perceived optically. When supplying HCl to the new iron dopant line, we could see some depositions on all ports of the reactor inlet flange and at the quartz/quartz junction at the gas lead chamber above a total flux of 60 sccm of total gas supply to this line (Fig. 3). From this fact we can conclude, that leakages occur at these positions as a result of the combination of dynamic pressure effects inside the quartz tube and insufficient gas tightness at the respective junctions. Due to the thermally and chemically very harsh conditions inside the reactor, it is not possible to apply proper sealings at these junctions. As a result, we had to limit the maximum gas flow through the ferrocene doping line to 60 sccm in all subsequent experiments.



**Fig. 3:** Photographs of the reactor inlets (left) and the quartz tube/gas-mixing chamber junction (right) during an ammonium-chloride haze experiment to determine the maximum possible flow inside the ferrocene doping channel. Bright lines are enclosing ammonium-chloride depositions.

**Table 1:** Overview on sample resistivities.

Bath temperature (°C)	Bath medium	Growth rate (%)	Ferrocene flow ( $\mu\text{mol min}^{-1}$ )	Resistivity ( $\Omega\text{cm}$ )
-	-	100	0	0.2
25	Water	100	0.03	0.35
60	Water	50	0.65	3.6
90	Ultra 350	100	2.6	2.1
90	Ultra 350	100	6.2	1.8
90	Ultra 350	50	6.2	1.4

The parameter the most influential on the amount of ferrocene transported to the reactor, is the temperature of the bubbler. While carrier gas flux and bubbler pressure have a linear influence, the vapor pressure and hence the material flux is exponentially dependent on the temperature of the respective material. The highest stable temperature that can be achieved inside our transport lines with the installed line heating is 95 °C. Therefore the bubbler temperature should be limited to 90 °C, else we risk ferrocene depositions inside the gas lines.

If we set all parameters to their respective limits (bubbler pressure to 950 hPa, bubbler temperature to 90 °C and total doping line flux to 60 sccm), taking into account a vapor pressure of 200 Pa for ferrocene at the given temperature [8], we get a calculated maximum molar flow of 6.2  $\mu\text{mol min}^{-1}$ .

#### 4. First Doping Experiments

Table 1 shows the resistivity results for the first experiments that we conducted with the new doping setup. The first line of this table shows the resistivity of an undoped sample as a reference. The following samples have been grown during different stages of the installation of the setup. With the progressing installation of the line heating, we were able to increase the bubbler temperature step by step. Before increasing the bath temperature from 60 °C to 90 °C, we exchanged the bath medium from water to *Lauda Ultra 350*. This is a toluol based liquid which can be used to operate the bath with temperatures of up to 150 °C. As we can see, the resistivity values increase with an increasing calculated molar flow of up to 0.65  $\mu\text{mol min}^{-1}$ , combined with a lower growth rate. For higher molar flows the resistivity decreases again. Lower growth rates seem to make things worse at these high ferrocene flow rates.

In order to exclude effects caused by premature decomposition of the ferrocene inside the reactor (see Sect. 2), we had a look at the short, 8 mm thick quartz pipe, transporting the ferrocene from the line into the reactor. Near the end of the small, inner quartz tube we could see a grey, transparent deposit (Fig. 4), most probably consisting of metallic iron. As a consequence, the 8 mm tube has been cut at the start of the grey deposits. By this we decrease the temperature at which we mix the ferrocene with the HCl gas, favoring the reaction of the ferrocene with HCl over thermal decomposition. However,

**Table 2:** SIMS sample overview.

Sample	Growth rate (%)	Ferrocene flow ( $\mu\text{mol min}^{-1}$ )	Growth temperature ( $^{\circ}\text{C}$ )	Resistivity ( $\Omega\text{cm}$ )
A	50	0.65	1050	3.6
B	50	2.6	1050	1.7
C	100	6.2	1050	1.8
D	100	2.6	1050	0.49
E	100	2.6	950	0.018
F	100	2.6	1100	0.62

comparing samples before and after the shortening of the glass tube, only a small increase in resistivity could be seen.



**Fig. 4:** Photograph of the 8 mm glass tube with iron deposits (inside the circle). The bright line marks the position of the shortening. The larger transport tube also shows some depositions.

As means to investigate the reasons for the low resistivity values at high ferrocene molar flows, we sent some samples to the Fraunhofer Institute for Applied Solid State Physics (IAF) in Freiburg, for secondary ion mass spectrometry (SIMS) of the iron concentration (Fig. 5). The Fe concentration near the surface of all analyzed samples approaches a value in the low  $10^{17} \text{ cm}^{-3}$  range. However, at the beginning of the ferrocene doped growth in HVPE, we can see a peak in the iron concentration. The drastic decline in the iron incorporation shortly after the maximum concentration may be due to local cooling of the solid ferrocene in the bubbler, caused by the hydrogen carrier gas entering the bubbler at room temperature. With a lower partial pressure, caused by the decreased temperature, the molar flow of the ferrocene drastically decreases, leading to a smaller iron concentration in the grown material.

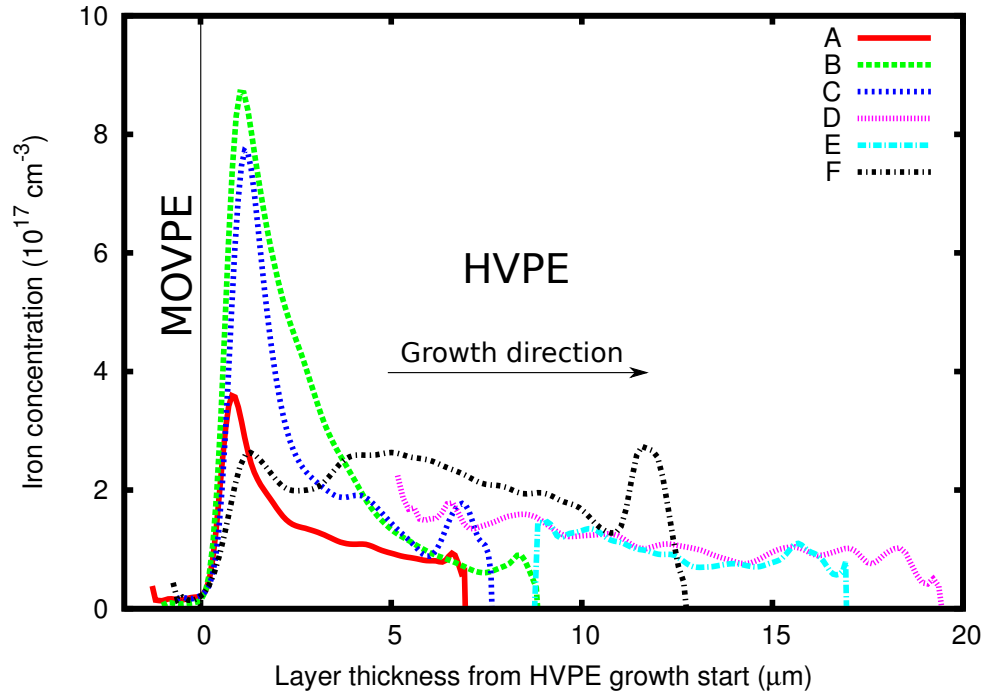


**Fig. 5:** SIMS profiles of the iron concentration of the samples from Table 2. Samples A–C are grown with different ferrocene molar flows, samples D–F are grown at different growth temperatures (see Table 2). The sample surface is situated at the right end of the measurement curve, the MOVPE-HVPE-GaN interface can be found at the  $x$ -axis origin.

In order to prevent this effect, we intend to preheat the carrier gas before it enters the bubbler. As a simple solution we have designed and ordered a gas line coil, that can be placed in the temperature-controlled bath, next to the bubbler. By using this device, the carrier gas will ideally be heated to the temperature of the bubbler.

## 5. Summary

A ferrocene doping line including a temperature controlled bubbler, a dilution setup, a heated transport line and modified quartz parts to securely transport this source gas species to the growth zone has been designed and put into service at our hydride vapor phase epitaxial machine. First experiments show, that in order to overcome the high unintentional doping levels in our thick GaN layers, we need a rather high ferrocene molar flow for compensation. To achieve the necessary high molar flows, a heated bubbler is essential. Most probably because of the low heat transfer of the powdery ferrocene inside the bubbler, high doping levels can only be achieved in the first few micrometers of ferrocene doped growth before the material is locally cooled down and the mass transport of the ferrocene is limited to a rather small level. In order to overcome this problem, we intend to preheat the carrier gas upstream of the bubbler. An appropriate device has been designed and ordered.

## Acknowledgment

I thank T. Meisch, J. Wang, M. Alimoradi-Jazi, D. Heinz and O. Rettig for their continuous effort to supply me with templates. I also thank AIXTRON SE, Aachen for planning and realizing the ferrocene doping line and L. Kirste from the Fraunhofer Institute of Applied Solid State Physics (IAF) in Freiburg for conducting SIMS measurements. This work was financially supported by the German Federal Ministry of Education and Research (BMBF) within the “TeleGaN” project.

## References

- [1] R. Mitova, R. Ghosh, U. Mhaskar, D. Klikic, M. Wang, and A. Dentella, “Investigations of 600-V GaN HEMT and GaN diode for power converter applications”, *IEEE Trans. Power Electron.*, vol. 29, pp. 2441–2452, 2014.
- [2] D.S. Lee, J.W. Chung, H. Wang, X. Gao, S. Guo, P. Fay, P. and T. Palacios, “245-GHz InAlN/GaN HEMTs with oxygen plasma treatment”, *IEEE Electron Dev. Lett.*, vol. 32, pp. 755–757, 2011.
- [3] M. Wu, J.H. Leach, X. Ni, X. Li, J. Xie, S. Dogan, U. Ozgur, H. Morkoc, T. Paskova, E. Preble, K.R. Evans, and C-Z. Lu, “InAlN/GaN heterostructure field-effect transistors on Fe-doped semi-insulating GaN substrates”, *J. Vac. Sci. Technol. B*, vol. 28, pp. 908–911, 2010.
- [4] F. Lipski, “Semi-insulating GaN by Fe-doping in hydride vapor phase epitaxy using a solid iron source”, *Annual Report 2010*, pp. 63–70, Ulm University, Institute of Optoelectronics.
- [5] S. Heikman, S. Keller, S.P. DenBaars, and U.K. Mishra, “Growth of Fe doped semi-insulating GaN by metalorganic chemical vapor deposition”, *Appl. Phys. Lett.*, vol. 81, pp. 439–441, 2002.
- [6] Y. Kumagai, H. Murakami, Y. Kangawa, and A. Koukitu, “Growth and characterization of thick GaN layers with high Fe doping”, *Phys. Status Solidi C*, vol. 2, pp. 2058–2061, 2005.
- [7] A. Bhattacharjee, A. Rooj, D. Roy, and M. Roy, “Thermal decomposition study of ferrocene  $[(C_5H_5)_2Fe]$ ”, *J. Exp. Phys.*, vol. 2014, pp. 513268-1–8, 2014.
- [8] M.J.S. Monte, L.M.N.B.F. Santos, M. Fulem, J.M.S. Fonseca, and C.A.D. Sousa, “New static apparatus and vapor pressure of reference materials: naphthalene, benzoic acid, benzophenone, and ferrocene”, *J. Chem. Eng. Data*, vol. 51, pp. 757–766, 2006.